Supplementary Information

Controlling Optoelectronic Properties of Carbazole-Phosphine Oxide Hosts by Short-Axis Substitution for Low-Voltage-Driving PHOLEDs

Weibo Yang,[a] *Zhensong Zhang,*[b] *Chunmiao Han,*[a] *Zhen Zhang,*[a] *Hui Xu,**[a] *Pengfei Yan,*[a] *Yi Zhao,**[b] *and Shiyong Liu*[b]

[a] Key Laboratory of Functional Inorganic Material Chemistry, Ministry of Education, Heilongjiang University, 74 Xuefu Road, Harbin 150080 (P. R. China)

[b] State Key Laboratory on Integrated Optoelectronics, College of Electronics Science and Engineering, Jilin University, 2699 Qianjin Street, Changchun 130012 (P. R. China)

Content

Experimental section

Materials and Instruments

All the reagents and solvents used for the synthesis of the compounds were purchased from Aldrich and Acros companies and used without further purification.

^{1}H NMR spectra were recorded using a Varian Mercury plus 400NB spectrometer relative to tetramethylsilane (TMS) as internal standard. Molecular masses were determined by a

FINNIGAN LCQ Electro-Spraying Ionization-Mass Spectrometry (ESI-MS), or a MALDI-TOF-MS. Elemental analyses were performed on a Vario EL III elemental analyzer. Absorption and photoluminescence (PL) emission spectra of the target compound were measured using a SHIMADZU UV-3150 spectrophotometer and a SHIMADZU RF-5301PC spectrophotometer, respectively. Thermogravimetric analysis (TGA) and differential scanning calorimetry (DSC) were performed on Shimadzu DSC-60A and DTG-60A thermal analyzers under nitrogen atmosphere at a heating rate of 10 °C min^{-1}. Cyclic voltammetric (CV) studies were conducted using an Eco Chemie B. V. AUTOLAB potentiostat in a typical three-electrode cell with a platinum sheet working electrode, a platinum wire counter electrode, and a silver/silver nitrate (Ag/Ag^{+}) reference electrode. All electrochemical experiments were carried out under a nitrogen atmosphere at room temperature in acetonitrile. Phosphorescence spectra were measured in dichloromethane using an Edinburgh FPLS 920 fluorescence spectrophotometer at 77 K cooling by liquid nitrogen with a delay of 300 μs using Time-Correlated Single Photon Counting (TCSPC) method with a microsecond pulsed Xenon light source for 10 μs-10 s lifetime measurement, the synchronization photomultiplier for signal collection and the Multi-Channel Scaling Mode of the PCS900 fast counter PC plug-in card for data processing.

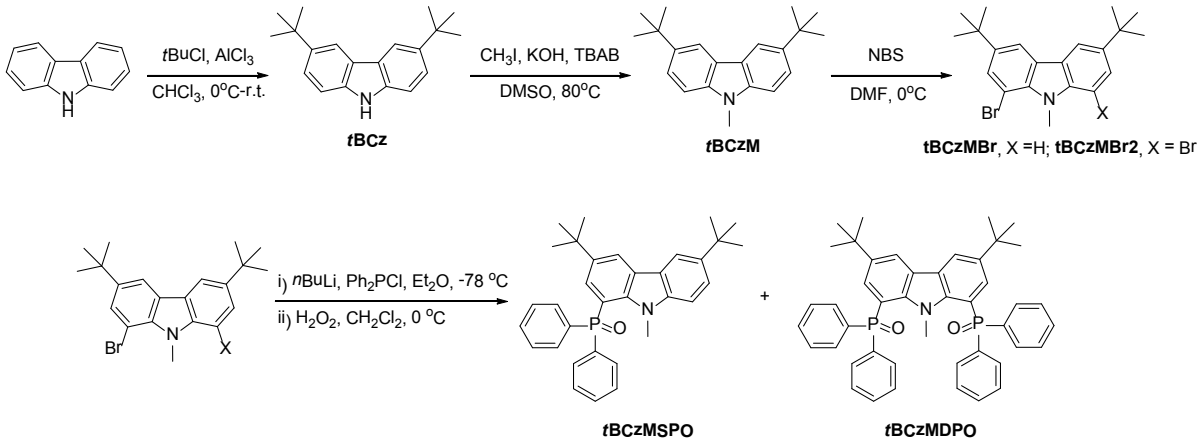

Scheme SI1. Synthetic routine of ***t*BCzMSPO** and ***t*BCzMDPO**.

Synthesis

*3,6-Di-tert-butyl-9H-carbazole (**tBuCz**)*: At 0 °C 16 g of $AlCl_3$ (120 mmol) was added in portions to a stirred solution of 20 g of carbazole (120 mmol) and 40 ml of *tert*-butyl chloride in 100 ml of $CHCl_3$. Then the mixture was stirred for 12 h. The reaction was quenched by lots of ice water, and extracted by dichloromethane (3 × 50 ml). The organic layer was dried with anhydride Na_2SO_4. The solvent was removed in *vacuo*. Then 120 ml of H_2SO_4 was added to the residue and stirred for 24 h. The reaction was quenched by lots of ice water, and extracted by dichloromethane (3 × 50 ml). The organic layer was dried with anhydride Na_2SO_4. The

residue was purified by flash column chromatography using petroleum ether/ethyl acetate (50:1) as eluent. Yield: 13.4 g of white powder (40%). ^{1}H NMR (TMS, $CDCl_3$, 400 MHz): δ = 8.117 (s, 2H), 7.852 (s, 1H), 7.490 (d, J = 8.4 Hz, 2H), 7.346 (d, J = 8.4 Hz, 2H), 1.489 ppm (s, 18H); GC-MS: m/z (%): 279 (100, $[M]^+$); elemental analysis (%) for $C_{20}H_{25}N$: C 85.97, H 9.02, N 5.01; found C 86.06, H 9.04, N 4.90.

*3,6-Di-tert-butyl-9-methyl-9H-carbazole (**tBCzM**)*: At room temperature 0.5 ml of KOH (50%, 8.95 mmol) was added to a stirred solution of 1.0 g of ***t*BuCz** (3.58 mmol) and 0.115 g of TBAB in 14 ml of DMSO. After stirred for half an hour, 0.33 ml of CH_3I (5.37 mmol) was added in dropwise. Then the mixture was warmed to 80 ^{o}C and stirred for 5h. The reaction was quenched by ice water, and extracted by dichloromethane (3 × 50 ml). The organic layer was dried with anhydride Na_2SO_4. The solvent was removed in *vacuo*. The organic layer was dried with anhydride Na_2SO_4. The residue was purified by purified by recrystallization using ethanol. Yield: 0.94 g of white powder (90%). ^{1}H NMR (TMS, $CDCl_3$, 400 MHz): δ = 8.130 (d, J = 1.6 Hz, 2H), 7.543 (dd, J_1 = 1.8 Hz, J_2 = 8.6 Hz, 2H), 7.324 (d, J = 8.4 Hz, 2H), 3.836 (s, 3H) , 1.489 ppm (s, 18H); GC-MS: m/z (%): 293 (100, $[M]^+$); elemental analysis (%) for $C_{21}H_{27}N$: C 85.95, H 9.27, N 4.77; found C 86.01, H 9.31, N 4.68.

*1-Bromo-3,6-di-tert-butyl-9-methyl-9H-carbazole (**tBCzMBr**)*: At 0 ^{o}C 1.33 g of NBS (7.5 mmol) was added in portions to a stirred solution of 2.0 g of ***t*BuCzM** (6.82 mmol) in 20 ml of DMF. Then the reaction mixture was warmed to room temperature and stirred for 12 h. The reaction was quenched by water, and extracted by dichloromethane (3 × 50 ml). The organic layer was dried with anhydride Na_2SO_4. The solvent was removed in *vacuo*, and the residue was purified by recrystallization using ethanol. Yield: 2.28 g of white powder (90%). ^{1}H NMR (TMS, $CDCl_3$, 400 MHz): δ = 8.036 (d, J = 1.6 Hz, 1H); 8.008 (d, J = 1.6 Hz, 1H); 7.595 (d, J = 1.6 Hz, 1H); 7.536 (q, J = 2.0 Hz, 8.8 Hz, 1H); 7.303 (d, J = 8.4 Hz, 1H); 4.179 (s, 3H); 1.428 ppm (d, J = 8.0 Hz, 18H); GC-MS: m/z (%): 371 (100, $[M]^+$), 373 (100, $[M+2]^+$); elemental analysis (%) for $C_{21}H_{26}NBr$: C 67.74, H 7.04, N 3.76; found C 67.83, H 7.09, N 3.84.

*1,8-Dibromo-3,6-di-tert-butyl-9-methyl-9H-carbazole (**tBCzMBr2**)*: This compound was prepared according to the same procedure of ***t*BCzMBr** from 2.0 g of ***t*BuCzM** with 2.05 equivalents of NBS. Yield: 2.76 g of white powder (90%). ^{1}H NMR (TMS, $CDCl_3$, 400 MHz): δ = 7.934 (d, J = 2.0 Hz, 2H), 7.639 (d, J = 1.6 Hz, 2H), 4.420 (s, 3H), 1.421 ppm (s, 18H); GC-MS: m/z (%): 451 (100, $[M+2]^+$), 449 (50, $[M]^+$), 453 (50, $[M+4]^+$); elemental analysis (%) for $C_{21}H_{25}NBr_2$: C 55.90, H 5.58, N 3.10; found C 55.92, H 5.62, N 3.17.

*3,6-Di-tert-butyl-1-(diphenylphosphoryl)-9-methyl-9H-carbazole (**tBCzMSPO**)*: At 0 ^{o}C 1.6 ml of n-BuLi (1.5 mmol) was added dropwise to a stirred solution of 1.0 g of ***t*BCzMBr** (2.68 mmol) in 20 ml of ether. The reaction mixture was stirred for 2h at 0 ^{o}C. Then 1.0 ml of Ph_2PCl was added to the mixture, and stirred overnight. The reaction was quenched by 20 ml of water, and extracted by dichloromethane (3 × 50ml). The organic layer was dried with anhydride Na_2SO_4. The solvent was removed in *vacuo*, and the residue was purified by flash column chromatography using dichloromethane as eluent and recrystallization using acetone. Yield: 0.8 g of white powder (60%). ^{1}H NMR (TMS, $CDCl_3$, 400 M Hz): δ = 8.277 (t, J = 1.8 Hz, 1H); 8.109 (d, J = 1.6 Hz, 1H); 8.144-8.088 (m, 4H) ; 7.584-7.496 (m, 3H) ; 7.430 (dt, J_1 = 2.8 Hz, J_2 = 7.4 Hz, 4H); 7.217 (d, J = 8.8 Hz, 1H); 7.073 (dd, J_1 = 2.0 Hz, J_2 = 17.6 Hz, 4H); 3.871 (s, 3H); 1.451 (s, 9H) ; 1.191 ppm (s, 9H); LDI-MS: m/z (%): 493 (100, $[M]^+$); elemental analysis (%) for $C_{33}H_{36}NOP$: C 80.30, H 7.35, N 2.84, O 3.24; found C 80.35, H 7.37, N 2.95, O 3.38.

*3,6-Di-tert-butyl-1,8-bis(diphenylphosphoryl)-9-methyl-9H-carbazole (**tBCzMDPO**)*: At -78 ^{o}C 7 ml of n-BuLi (17.6 mmol) was added dropwise to a stirred solution of 2.0 g of ***t*BCzMBr2** (4.4 mmol) in 150 ml of ether. The reaction mixture was stirred for 3 h at -78 ^{o}C. Then 3.6 ml of Ph_2PCl was added to the mixture, and stirred overnight. The reaction was quenched by 50 ml of water, and extracted by dichloromethane (3 × 50ml). The organic layer was dried with anhydride Na_2SO_4. The solvent was removed in *vacuo*, and the residue was purified by flash column chromatography using dichloromethane as eluent and recrystallization using acetone. Yield: 1.7 g of white powder (55%). ^{1}H NMR (TMS, $CDCl_3$, 400 M Hz): δ = 8.253 (t, J = 1.8 Hz, 1H), 7.617-7.541 (m, 8H) , 7.474 (dt, J_1 = 1.2 Hz, J_2 = 7.8 Hz, 4H), 7.371 (dt, J_1 = 2.8 Hz, J_2 = 7.8 Hz, 8H), 4.038 (s, 3H), 1.170 ppm (s, 18H); LDI-MS: m/z (%): 693 (100, $[M]^+$); elemental analysis (%) for $C_{45}H_{45}NO_2P_2$: C 77.90, H 6.54, N 2.02, O 4.61; found C 77.89, H 6.50, N 2.14, O 4.73.

Gaussian Calculations

Computations on the electronic ground states and triplet states of the single-molecular compounds in *vacuum* were performed using Becke's three-parameter density functional in combination with the nonlocal correlation functional of Lee, Yang, and Parr (B3LYP).[1,2] 6-31G(d) basis sets were employed. The ground-state geometries were fully optimized at the B3LYP level. All computations were performed using the Gaussian 03 package.[3]

Device Fabrication and Testing

The OLEDs with configurations of ITO|MoO_x (2 nm)|*m*-MTDATA:MoO_x (15 wt.%, 30 nm)|*m*-MTDATA (10 nm)|$Ir(ppz)_3$ (10 nm)|**Host** : Dopants (10 nm)| 3TPYMB (y nm)|Bphen

(40-y nm)|Cs_2CO_3 (1 nm)|Al were fabricated, where MoO_3 and Cs_2CO_3 served as hole- and electron-injecting layers, *m*-MTDATA is 4,4',4''-tri(*N*-3-methylphenyl-*N*-phenylamino)triphenylamine as the hole-transporting layer (HTL), $Ir(ppz)_3$ is tris(phenylpyrazole)iridium as hole-transporting/electron-blocking layer and BPhen is 4,7-diphenyl-1,10-phenanthroline as electron-transporting hole-blocking layer. For blue, green, yellow and red emitting devices, bis(4,6-(difluorophenyl)pyridinato-N,C2)picolinate iridium(III) (FIrpic), tris(2-phenylpyridine) iridium(III) ($Ir(ppy)_3$), iridium(III)bis(4-phenylthieno[3,2-c]pyridinato-N,C^2) acetylacetonate (PO-01) and bis(2-methyldibenzo[f,h]quinoxaline)(acetylacetonate) iridium (III) ($Ir(MDQ)_2acac$) were used as the dopants with the concentrations of 10, 8, 6 and 10%, respectively. Device **BA**, **BB**, **GA**, **YA** and **RA** were based on ***t*BCzMSPO**, and **BC**, **BD**, **GB**, **YB** and **RB** were on the basis of ***t*BCzMDPO**. For **BB** and **BD**, y was 10. For other devices, y was 0. The hole-only and electron-only devices were fabricated with the structures of ITO|MoO_x (2 nm)|*m*-MTDATA:MoO_x (15 wt.%, 30 nm)|*m*-MTDATA (10 nm)|$Ir(ppz)_3$ (10 nm)|**Host** (30 nm)|$Ir(ppz)_3$ (10 nm)|*m*-MTDATA (10 nm)|*m*-MTDATA:MoO_x (15 wt.%, 30 nm)|MoO_3 (2 nm)|Al and Al|Cs_2CO_3 (1 nm)|BPhen (40 nm)|**Host** (30nm)|BPhen (40 nm)|Cs_2CO_3 (1 nm)|Al, respectively. Prior to the device fabrication, the patterned ITO-coated glass substrates were scrubbed and sonicated consecutively with acetone, ethanol, and de-ionized water, respectively. All the organic layers were thermally deposited in vacuum (~4.0×10^{-4} Pa) at a rate of 1-2 Å/s monitored in situ with the quartz oscillator. In order to reduce the ohmic loss, a heavily p-doped layer with MoO_x, considering the low doping efficiency in amorphous organic matrix with transition-metal-oxide-based acceptors, was directly deposited onto the ITO substrate for each sample. After the deposition of Cs_2CO_3, the samples were transferred to metal chamber, and suffered from a vacuum break due to the change of the shadow masks to determine the active area. The current-voltage-luminance characteristics were measured with a PR650 spectrascan spectrometer and a Keithley 2400 programmable voltage-current source. All the samples were measured directly after fabrication without encapsulation in ambient atmosphere at room temperature.

Diagram of Energy Levels and EL Spectra of the Devices

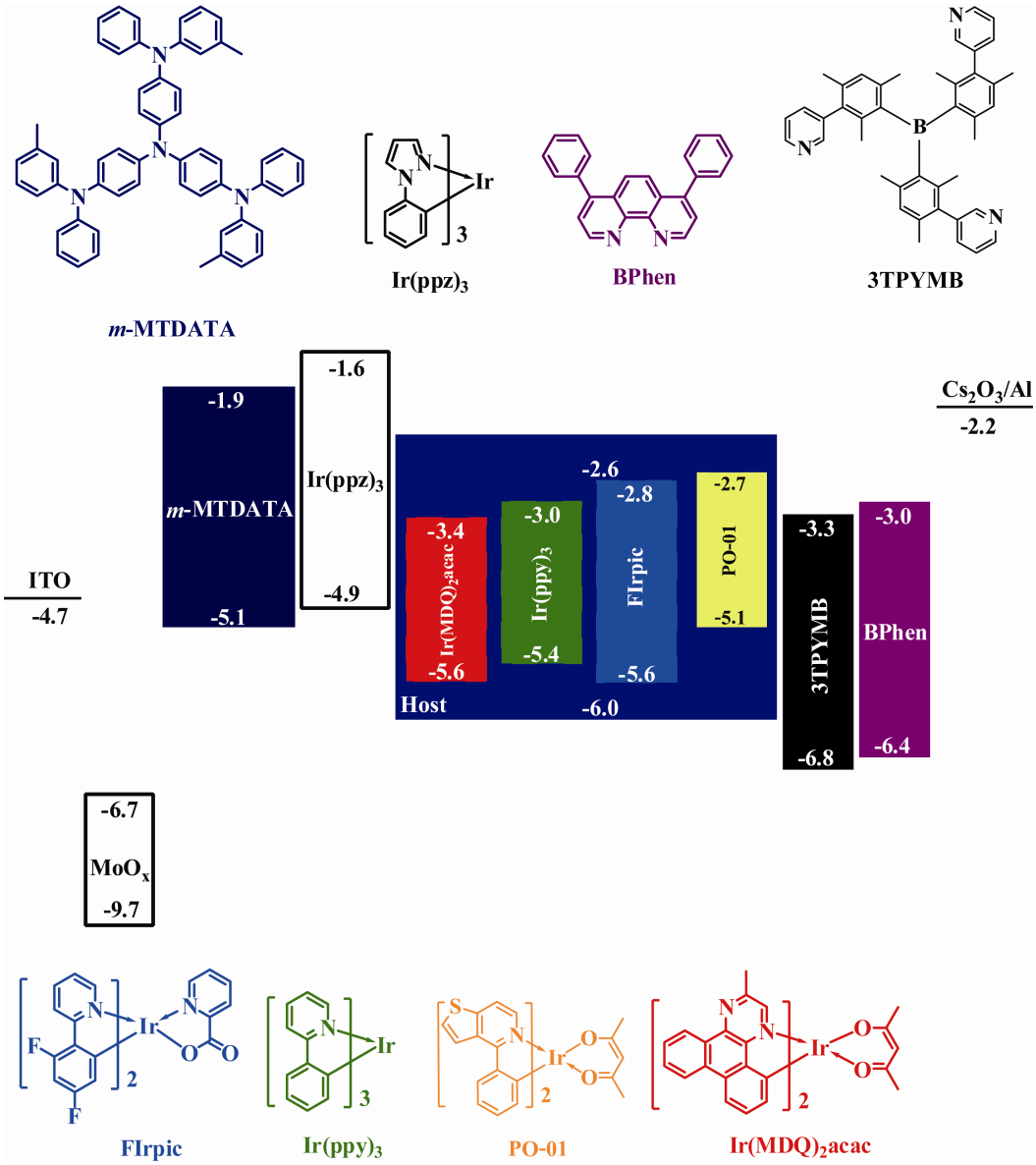

Scheme SI2. Energy level diagram of devices.

Thermal Properties

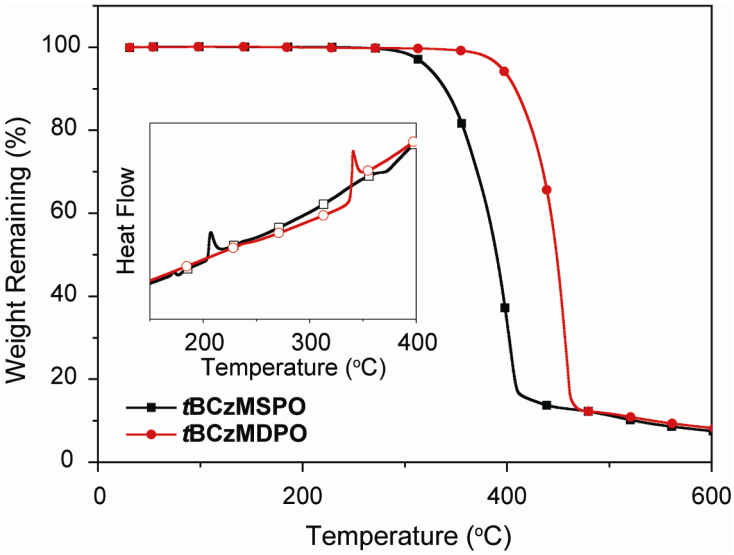

Figure SI1. TGA and DSC curves of ***t*BCzMxPO**.

Morphological Properties of the Thin Films

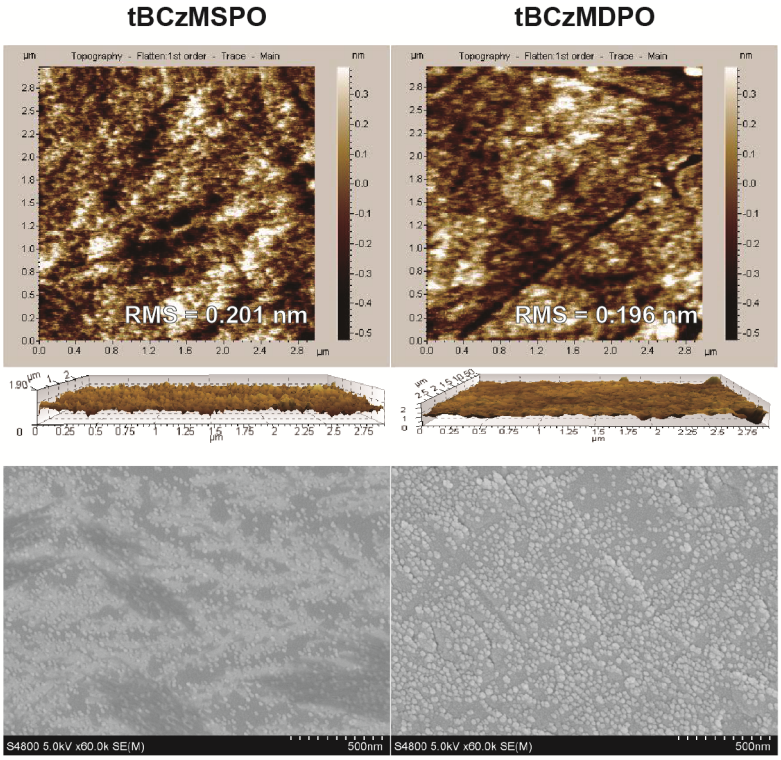

Figure SI2. AFM and SEM images of the thin films of ***t*BCzMSPO** and ***t*BCzMDPO**.

Time Decay Curves of *t*BCzMxPO in Solution

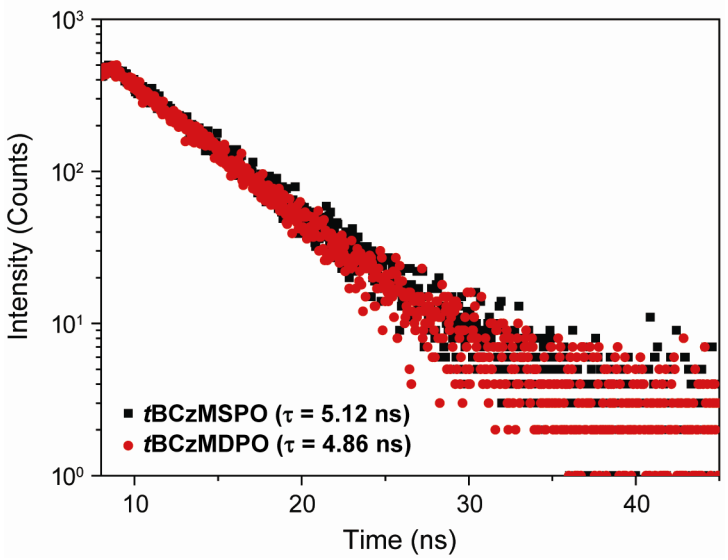

Figure SI3. Time Decay Curves of ***t*BCzMxPO** in Solution.

Optical Properties of *t*BCzM in Solution and Film

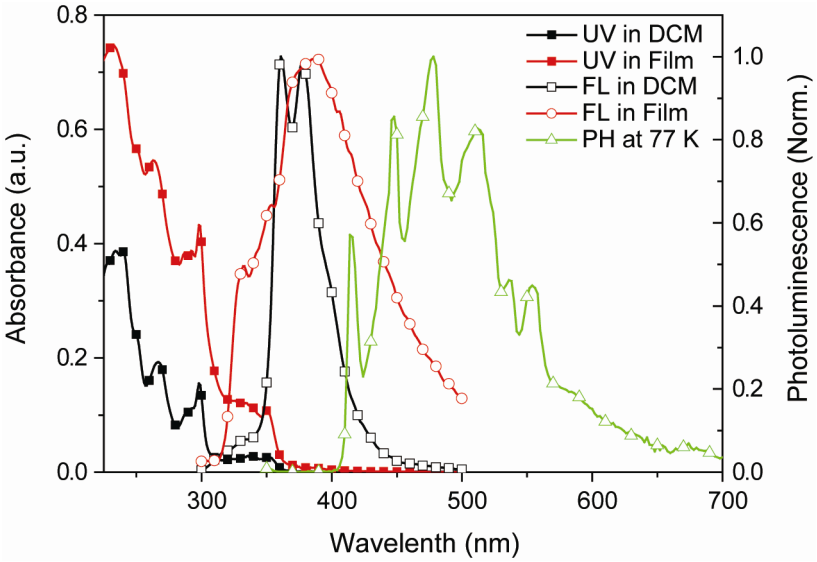

Figure SI4. Absorption and PL spectra of ***t*BCzM** in CH_2Cl_2 (10^{-6} mol L^{-1}) and film.

Optical Properties in Film

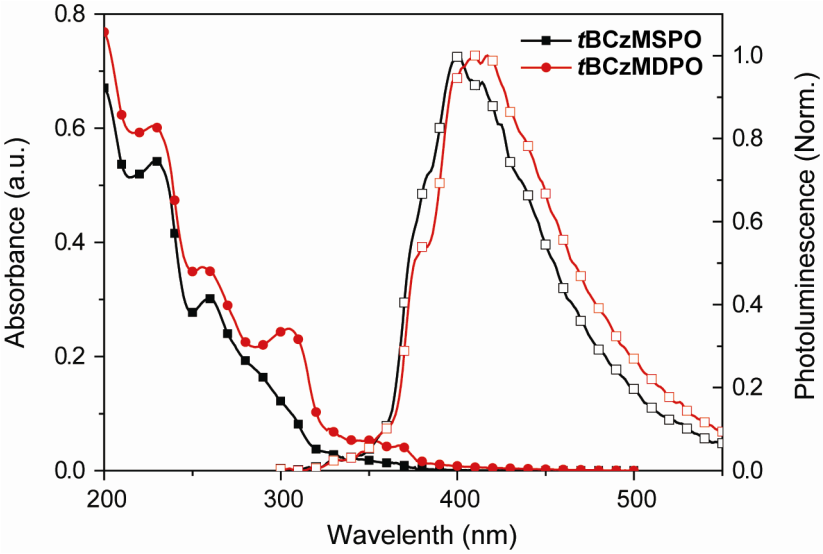

Figure SI5. Absorption and PL spectra of ***t*BCzMxPO** in film.

Solvent Effect on Emission of *t*BCzxPO

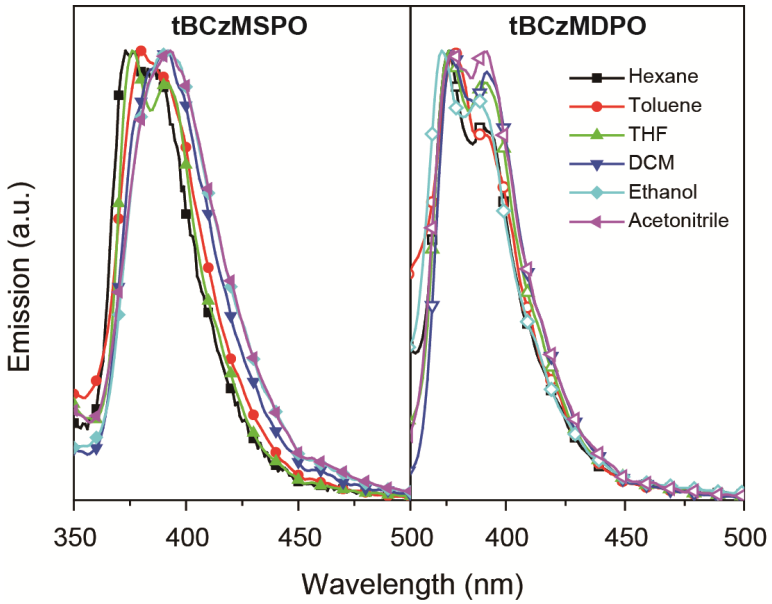

Figure SI6. PL spectra of ***t*BCzMxPO** in solvents with different polarities.

CV Analysis of *t*BCzMxPO

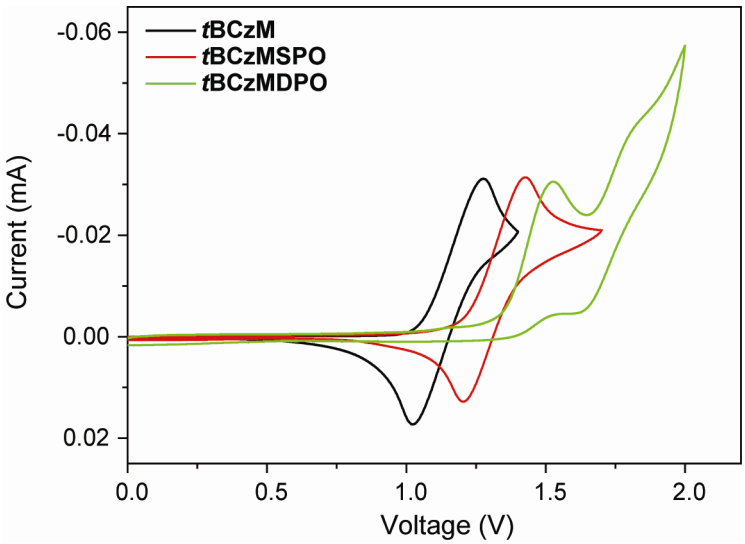

Figure SI7. Oxidation curves of ***t*BCzM** and ***t*BCzMxPO**.

IV Characteristics of Hole and Electron-Only Device of PO Hosts

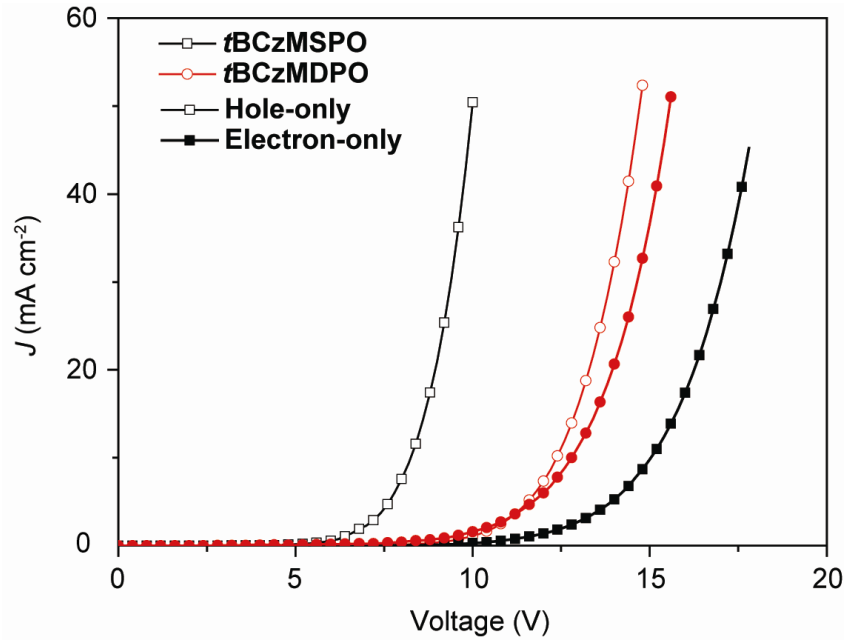

Figure SI8. IV curves of the single carrier-transporting devices of PO hosts.

Table SI1. Physical properties of the carbazole derivatives.

Compound	Absorption Peak (nm)	Emission Peak (nm)	HOMO/LUMO (eV)	S_1/T_1 (eV)	$T_g/T_m/T_d$ (°C)
***t*BCzM**	351, 339, 298, 267, 250, 240 [a] 351, 336, 298, 263, 250, 232 [b]	361, 377 [a] 388 [b]	-5.85 [c]/-2.41 [d] -5.09/0.57 [e]	3.44 [d]/2.98 [f] 4.52/- [e]	-/-/-
***t*BCzMSPO**	363, 351, 306, 288, 254, 228 [a] 366, 300, 261, 229 [b]	391 [a] 383, 400 [b]	-5.99 [c]/-2.63 [d] -5.22/-0.87 [e]	3.36 [d]/2.98 [f] 4.35/2.98 [e]	175/206/323
***t*BCzMDPO**	366, 351, 306, 253, 228 [a] 369, 355, 306, 256, 228 [b]	382, 393 [a] 380, 409 [b]	-6.13 [c]/-2.87 [d] -5.31/-1.01 [e]	3.26d/2.98 [f] 4.30/2.98 [e]	-/340/394

[a] In DCM (10^{-6} mol L^{-1}); [b] in film; [c] calculated from the onset oxidation voltages in CV curves; [d] estimated from the experimental HOMOs and absorption edges; [e] the simulated results from DFT calculation; [f] estimated from the 0-0 transitions in phosphorescence spectra.

Table SI2. EL performance of the hosts for PHOLEDs.

Device	Operating Voltage (V)[a]	Maximum Efficiencies[b]	Efficiency Roll-Offs (%)[c]		
			C.E.	P.E.	E.Q.E.
BA	2.6, <3.2, <4.2	16.0, 16.8, 8.7	15, 48	20, 63	15, 48
BB	2.6, <3.2, <4.2	20.2, 19.2, 11.0	13, 47	18, 62	13, 46
BC	2.6, <3.2, <4.4	7.9, 8.9, 4.3	16, 54	27, 71	16, 56
BD	2.6, <3.2, <4.4	8.9, 9.8, 4.9	17, 60	28, 76	16, 59
GA	2.6, <3.0, <3.4	33.2, 34.7, 9.7	-, 12	-, 22	-, 11
GB	2.6, <3.0, <3.4	22.3, 23.4, 6.7	-, 12	-, 22	-, 12
YA	3.0, <3.4, <4.0	17.6, 17.2, 5.4	10, 28	15, 42	9, 28
YB	2.6, <2.8, <3.4	12.2, 13.6, 3.8	-, 17	-, 32	-, 18
RA	3.0, <5.0, <7.0	3.0, 2.6, 1.7	23, 60	46, 80	24, 59
RB	3.0, <5.2, <7.0	1.3, 1.1, 0.9	0, 23	27, 55	9, 22

[a] In the order of onset, 100 and 1000 cd m^{-2}; [b] in the order of C.E. (cd A^{-1}), P.E. (lm W^{-1}) and E.Q.E. (%); c in the order of 100 and 1000 cd m^{-2}.

EL Performance of Green, Yellow and Red PHOLEDs

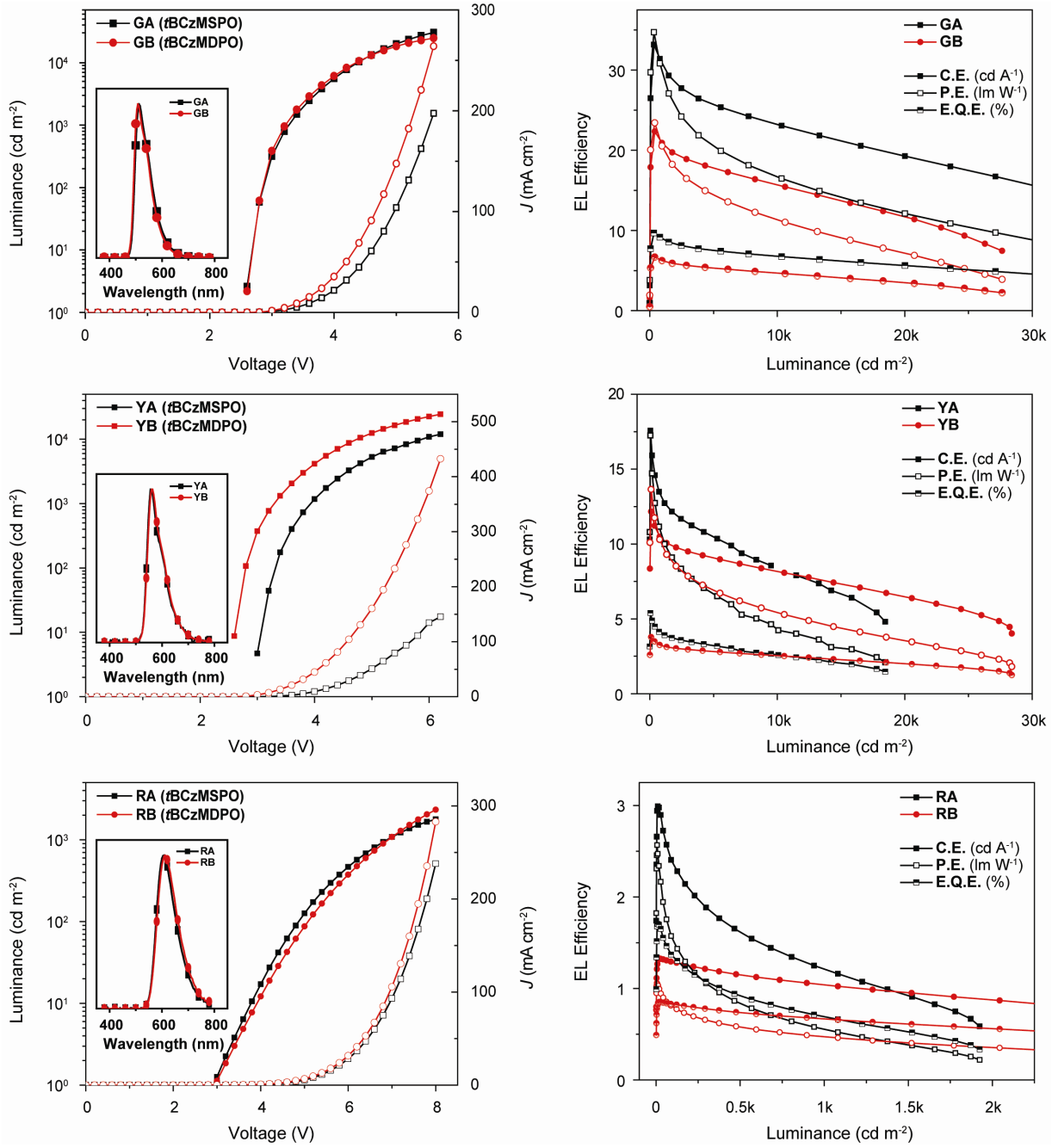

Figure SI9. Brightness-*J*-voltage and efficiency curves of green, yellow and red PHOLEDs.

Reference

[1] D. Becke, *J. Chem. Phys.* **1993**, *98*, 5648-5652.

[2] Lee,; W. Yang,; R. G. Parr, *Phys. Rev. B* **1988**, *37*, 785-789.

[3] M. J. Frisch, G. W. Trucks, H. B. Schlegel, G. E. Scuseria, M. A. Robb, J. R. Cheeseman,

J. A. Montgomery, Jr., T. Vreyen, K. N. Kudin, J. C. Burant, J. M. Millam, S. S. Iyengar, J. Tomasi, V. Barone, B. Mennucci, M. Cossi, G. Scalmani, N. Rega, G. A. Petersson, H. Nakatsuji, M. Hada, M. Ehara, K. Toyota, R. Fukuda, J. Hasegawa, M. Ishida, T. Nakajima, Y. Honda, O. Kitao, H. Nakai, M. Klene, X. Li, J. E. Knox, H. P. Hratchian, J. B. Cross C. Adamo, J. Jaramillo, R. Gomperts, R. E. Stratmann, O. Yazyev, A. J. Austin, R. Cammi, C. Pomelli, J. W. Octhterski, P. Y. Ayala, K. Morokuma, G. A. Voth, P. Salvador, J. J. Dannenberg, V. G. Zakrzewski, S. Dapprich, A. D. Daniels, M. C. Strain, O. Farkas, D. K. Malick, A. D. Rabuck, K. Raghavachari, J. B. Foresman, J. V. Ortiz, Q. Cui, A. G. Baboul, S. Clifford, J. Cioslowski, B. B. Stefanov,G. Liu,A. Liashenko, P. Piskorz, I. Komaromi, R. L.Martin, D. J. Fox, T. Keith, M. A. Al-Laham, C. Y. Peng, A.Nanayakkara,M. Challacombe, P.M.W.Gill, B. Johnson,W. Chen, M.W.Wong, C. Gonzalez and J. A. Pople, Gaussian 03, Revision D.02, Gaussian, Inc., Pittsburgh, PA, **2004**.